Electronic Supporting Information

Stretchable energy harvesting devices: attempts to high-performance electrodes

Codrin Tugui, Cristian Ursu, Liviu Sacarescu, Mihai Asandulesa, George Stoian, Gabriel Ababei, Maria Cazacu

This file contains:

Figures S1-S18

Pages S1-S10

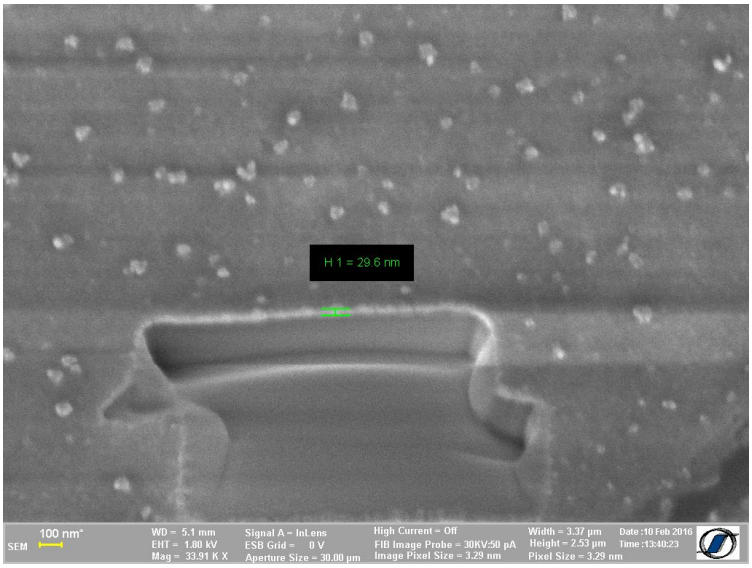

Figure S1. FIB-SEM image of silver electrode deposed on silicone dielectric.

The dependence between the scattering intensity I(q) and wave vector q can be correlated with the components dimension in the sample.[1] In some cases, because of certain shortcomings related with the polydispersity or shape, the SAXS analysis should be performed based on mathematical models (Figure S1).[2] The model describing the studied system was built using the "Beaucage unified field" fitting method at two levels: primary particles (level 1) and aggregates (level 2). The calculations were done using the software "Irena: tool suite for modelling and analysis of small-angle scattering".[3]

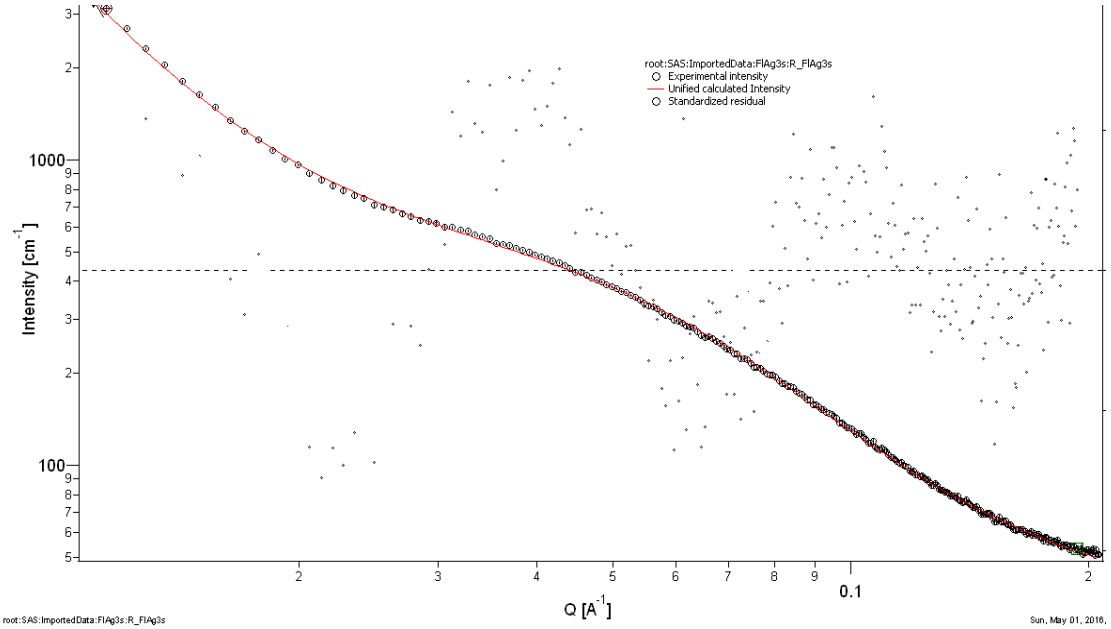

Figure S2. SAXS scattering curve.

Level 1 parameters: Guinier factor, G=508.75; radius of gyration, Rg= 25.27 Å; Porod exponent, P=3.05

Level 2 parameters: G=0; B= 0.0093946; Porod exponent, P=2.77.

Considering the estimated gyration radius and assuming a globular shape (Porod exponent P=3) it can be determined the average dimension of the primary particles (Guinier relation), Dmax=2.58 x Rg and Rg=65 Å.

Next, the correlation length was calculated based on the fractal model. Thus, an interparticle distance within the aggregates of about 22 Å (K_{Si} in the inset) was obtained.

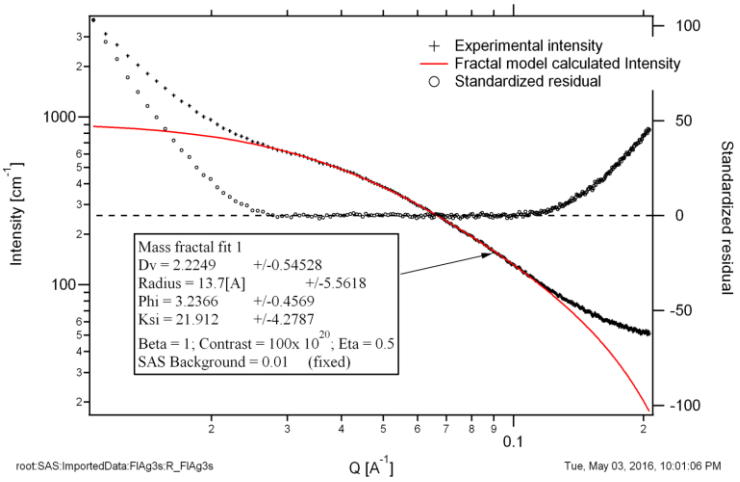

Figure S3. Fitting plot of fractal model.

Figure S4. Equiaxial stretching setup.

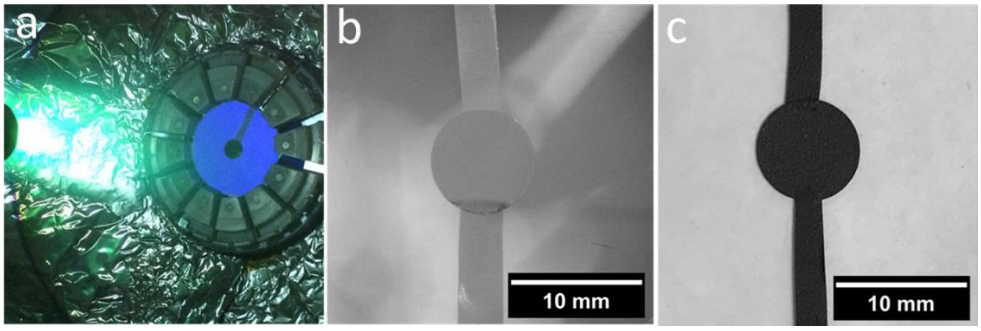

Figure S5. a) Image during deposition of silver electrode; b) silver electrode deposited on DE used in actuation measurements; c) PDMS-Cb electrode attached on DE used in actuation measurements.

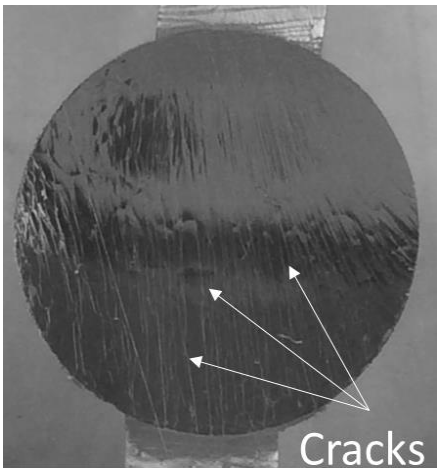

Figure S6. Image of actuated silver electrode.

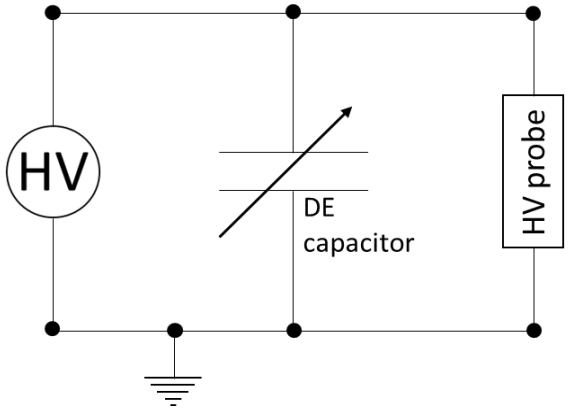

Figure S7. Schematic representation of the energy harvesting setup.

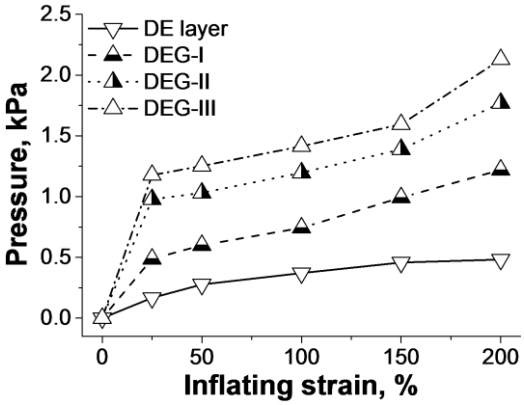

Figure S8. Pressure needed to inflate the DEG, depending on the number of dielectric layers.

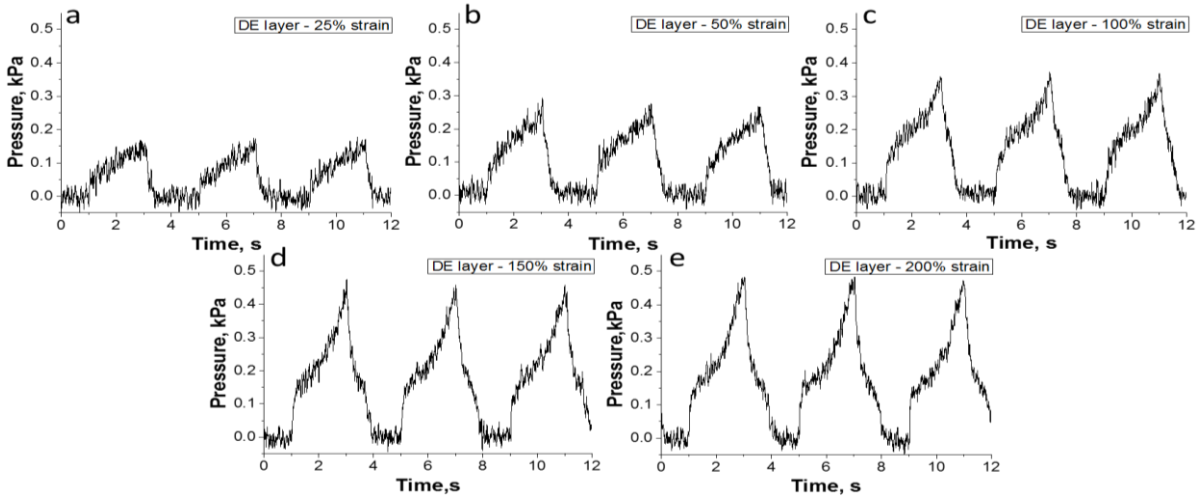

Figure S9. Inside air chamber pressure during harvesting cycles of a single DE layer.

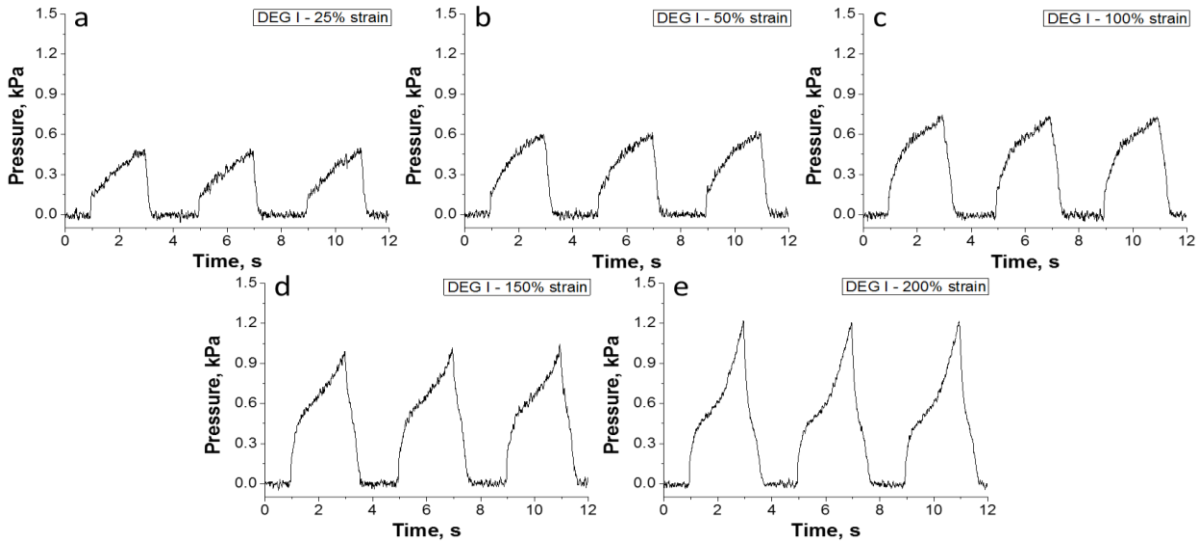

Figure S10. Inside air chamber pressure during harvesting cycles of DEG I.

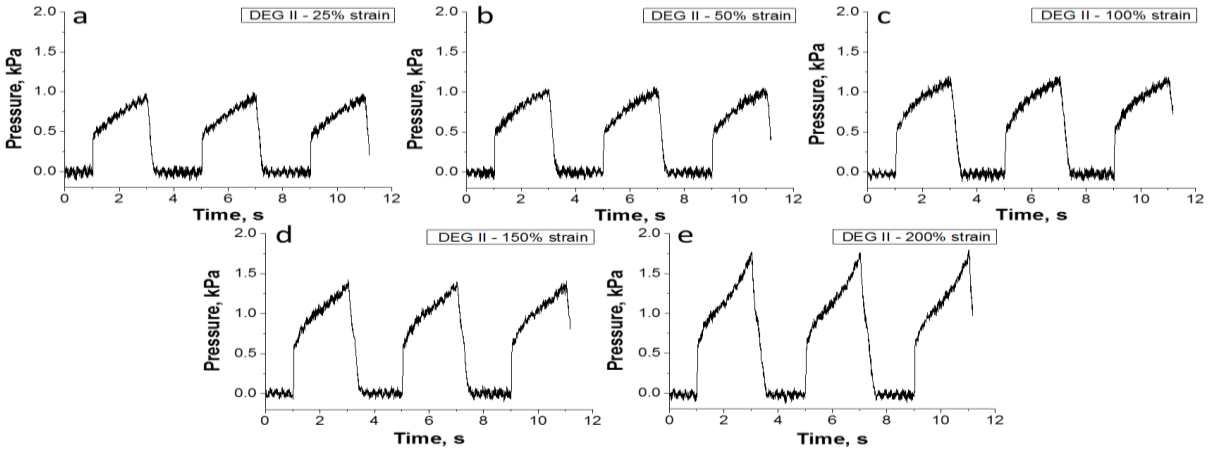

Figure S11. Inside air chamber pressure during harvesting cycles of DEG II.

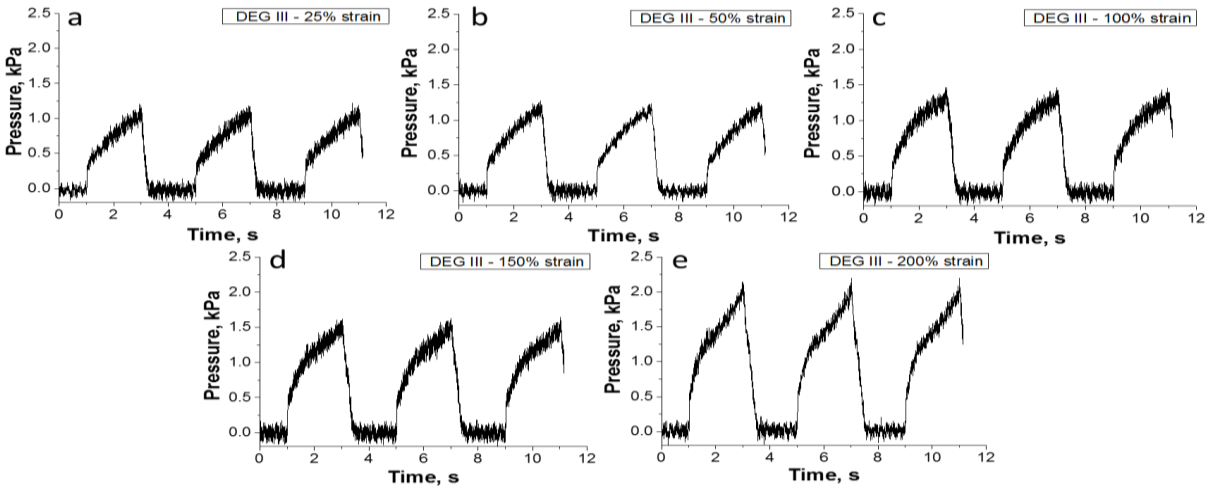

Figure S12. Inside air chamber pressure during harvesting cycles of DEG III.

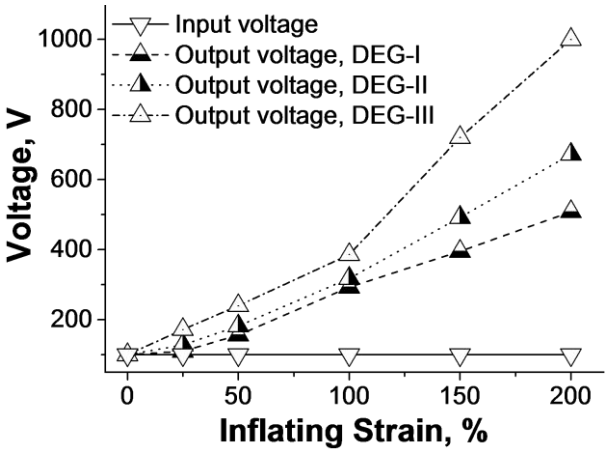

Figure S13. Measured output voltage and inflating pressure as a function of inflating strain, U_{input}=100V.

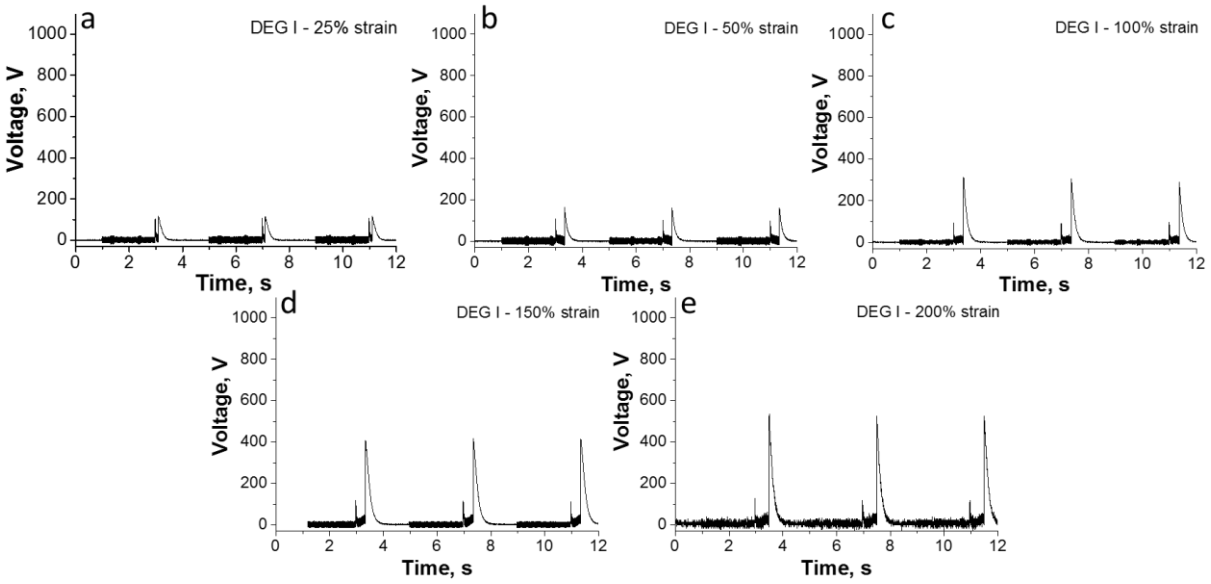

Figure S14. Harvested voltage of DEG I.

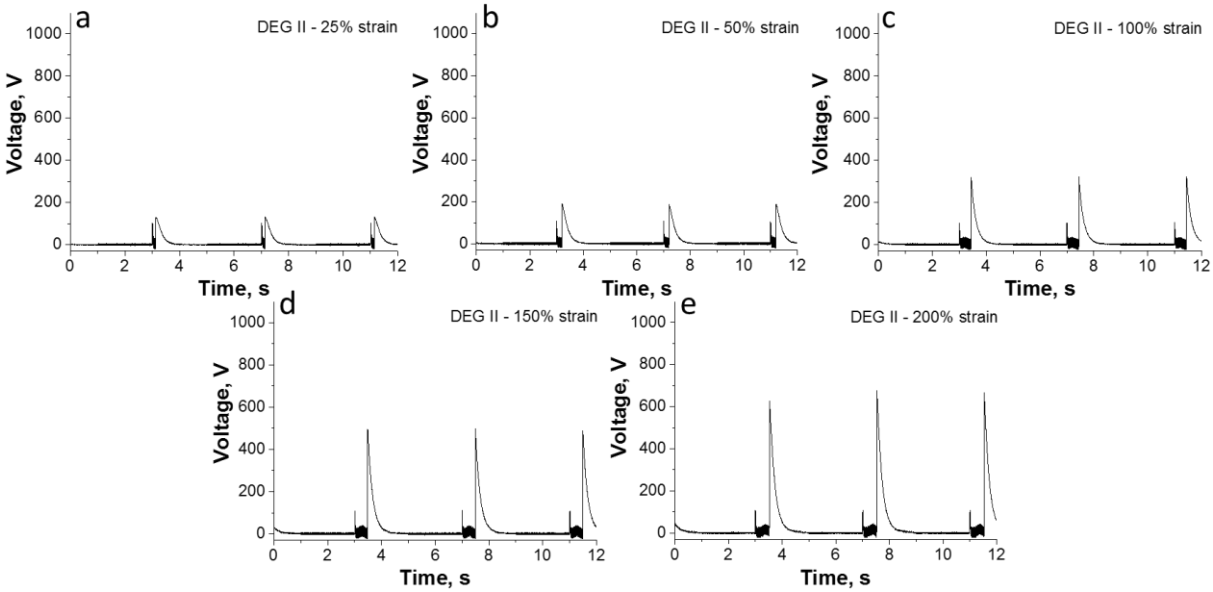

Figure S15. Harvested voltage of DEG II.

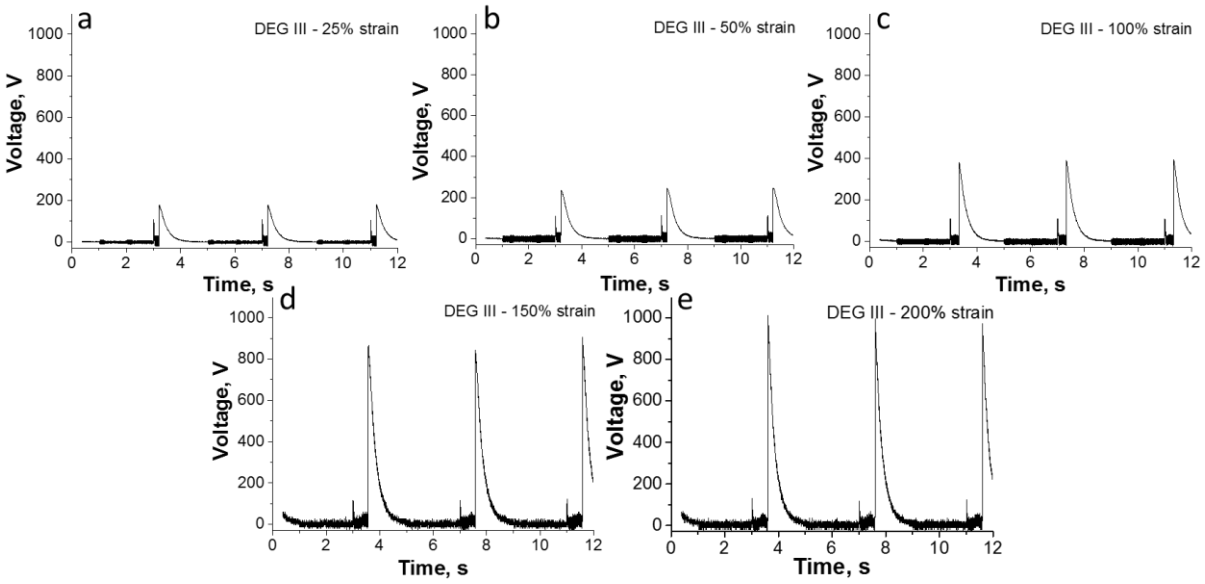

Figure S16. Harvested voltage of DEG III.

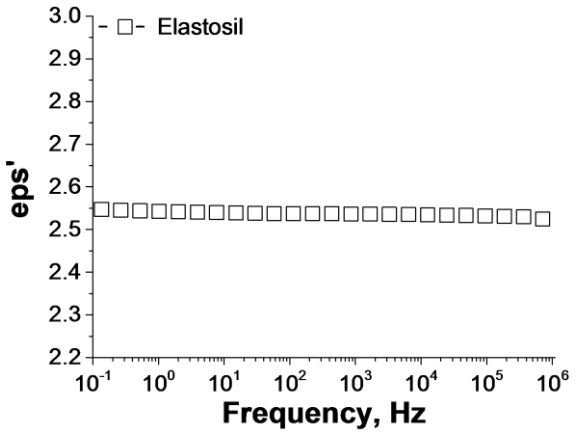

Figure S17. Dielectric spectrum of DE.

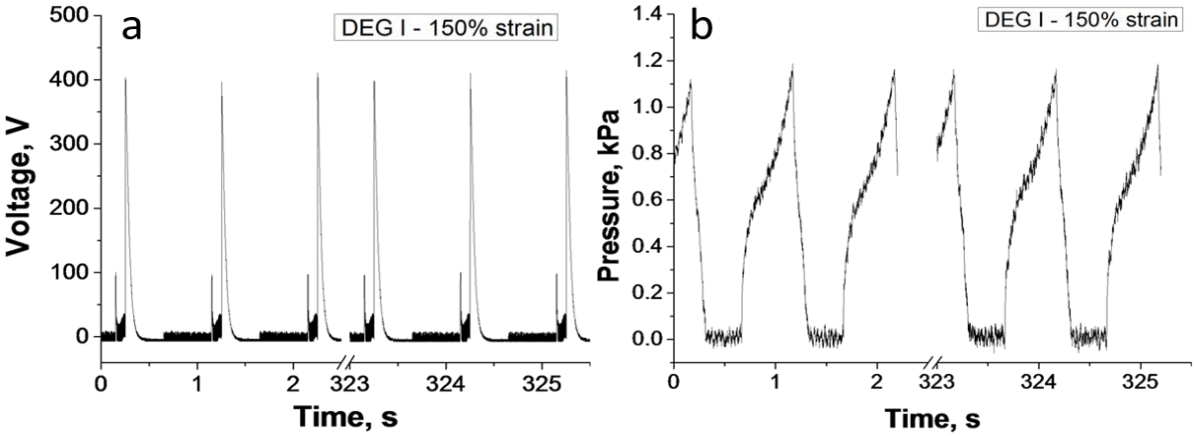

Figure S18. Variation of harvested voltage **(a)** and air chamber pressure **(b)** depending on the number of cycles.

References

(1) Suryawanshi, C. N.; Pakdel, P.; Schaefer, D. W. Effect of Drying on the Structure and Dispersion of Precipitated Silica. *J. Appl. Crystallogr.* **2003**, *36*, 573–577.

(2) Beaucage, G. Approximations Leading to a Unified Exponential Power-Law Approach to Small-Angle Scattering. *J. Appl. Crystallogr.* **1995**, *28*, 717–728.

(3) Ilavsky, J.; Jemian, P. R. Irena: Tool Suite for Modeling and Analysis of Small-Angle Scattering. *J. Appl. Crystallogr.* **2009**, *42* (2), 347–353.